Centromere protein W promotes epithelial-mesenchymal transition in liver cancer via the Hippo-YAP signaling pathway

XIA FENG[1,2], YINGHUI WANG[2], LINGLING WANG[3], HAIXIA YANG[2], YUNLU QIN[4], JIANYONG ZHOU[2] and FANG YU[1]

[1]School of Medical Laboratory, Guizhou Medical University, Guiyang, Guizhou 550004, P.R. China; [2]Department of Clinical Laboratory, Qiannan People's Hospital, The First Affiliated Hospital of Qiannan National Medical College, Duyun, Guizhou 558003, P.R. China; [3]Department of Pathology, Qiannan People's Hospital, The First Affiliated Hospital of Qiannan National Medical College, Duyun, Guizhou 558003, P.R. China; [4]Department of Medical Laboratory, Qiannan National Medical College, Duyun, Guizhou 558013, P.R. China

Received April 8, 2026; Accepted November 2, 2026

DOI: 10.3892/ol.2026.15968

Abstract. Liver cancer is a highly lethal malignancy with limited therapeutic options. The aim of the present study was to investigate the expression, biological function and underlying mechanism of centromere protein W (CENPW) in liver cancer and its association with the Hippo-Yes-associated protein (YAP) signaling pathway. Bioinformatic analyses using TIMER2.0 and The Cancer Genome Atlas databases revealed that CENPW expression was upregulated in multiple cancer types, including liver cancer, and that high CENPW expression was associated with shorter overall survival time in patients with liver cancer. These results were further validated by immunohistochemistry, reverse transcription-quantitative PCR and western blot analysis in liver cancer tissues and cell lines. Functional assays demonstrated that CENPW knockdown inhibited the proliferation, migration and invasion of liver cancer cells; induced apoptosis and S-phase cell cycle arrest; and suppressed epithelial-mesenchymal transition (EMT), as indicated by increased E-cadherin expression and decreased N-cadherin expression. Mechanistically, CENPW knockdown promoted YAP phosphorylation and increased the phosphorylated-YAP/YAP ratio, indicating decreased YAP activity. Pharmacological reactivation of YAP signaling using the large tumor suppressor kinase inhibitor TRULI partially reversed the suppression of EMT and restored the migratory and invasive abilities of CENPW-silenced cells. In conclusion, the present study revealed that CENPW may be a promoter of malignant phenotypes in liver cancer and that its oncogenic functions can be at least partially mediated through regulation of the Hippo-YAP signaling pathway. Therefore, CENPW may serve as a biomarker and therapeutic target for liver cancer.

Correspondence to: Dr Fang Yu, School of Medical Laboratory, Guizhou Medical University, 9 Beijing Road, Yunyan, Guiyang, Guizhou 550004, P.R. China
E-mail: yu.fang@gmc.edu.cn

Key words: centromeric protein W, liver cancer, Hippo-Yes-associated protein signaling, epithelial-mesenchymal transition, tumor progression

Introduction

Liver cancer represents a major global health burden, particularly in regions with a high prevalence of liver disease,ranking as the sixth most frequently diagnosed malignancy and the thirdleading cause of cancerrelated death worldwide, with ~866 000 new cases and 759 000 livercancerassociated deaths reported annually (1). Although advances in surgical resection, chemotherapy and targeted therapy have improved treatment options (2), the prognosis of patients with liver cancer remains poor, with 5-year net survival rates ranging from 3 to 30% across countries worldwide, and an overall 5-year relative survival of ~21% among adults in the United States, due to limitations in early diagnosis and effective control of tumor progression and metastasis (3,4). Therefore, identifying novel molecular regulators involved in liver cancer development is essential for improving therapeutic strategies.

Centromere protein (CENP) W, also known as cancer upregulated gene 2 (CUG2), is a component of the constitutive centromere-associated network and forms a complex with CENPT (5,6), playing key roles in kinetochore function and chromosome separation during mitosis (7,8). Proteins in this family constitute the centromere-kinetochore complex. Dysregulation of centromere-associated proteins has been repeatedly linked to tumorigenesis, and aberrant upregulation of numerous CENP family members has been documented across diverse malignancies (9-13).

Previous studies have shown that CENPW is upregulated in liver cancer, is associated with poor prognosis and that its knockdown suppresses proliferation, migration and invasion while inducing apoptosis and cell cycle arrest (14,15). Additionally, a comprehensive review has summarized the oncogenic characteristics of various centromere protein members in hepatocellular carcinoma (16). Multiomics analysis combining single-cell transcriptomics, weighted gene co-expression analysis and machine learning further identified CENPW as a critical hub biomarker that is upregulated in liver cancer (17). However, the downstream signaling mechanisms

through which CENPW promotes malignant phenotypes in liver cancer remain incompletely understood.

The Hippo signaling pathway is a central regulator of liver homeostasis and tumorigenesis, with Yes-associated protein 1 (YAP1) acting as a key downstream effector (18,19). Aberrant activation of YAP1 is frequently observed in liver cancer and contributes to tumor growth, epithelial-mesenchymal transition (EMT), invasion and metastasi (20). Notably, CENPW has been reported to promote EMT in lung cancer cells by increasing YAP1 activity (21), suggesting a potential functional link between CENPW and Hippo-YAP signaling. However, whether CENPW regulates liver cancer progression through this pathway remains unclear.

The present study investigated the expression and biological function of CENPW in liver cancer and explored its potential association with Hippo-YAP signaling. These findings may provide new insight into the role of CENPW in regulating liver cancer cell proliferation, EMT and malignant progression.

Materials and methods

Patients and tissue samples. In total, 5 fresh and 15 paraffin-embedded liver cancer tissue samples, together with matched adjacent non-tumorous liver tissue samples, were collected at Qiannan People's Hospital (Duyun, China) for the present study, following ethical approval granted by the Ethics Committee of Qiannan People's Hospital (Duyun, China; approval no. 2025-qnzy-13). Sample collection and archive retrieval were performed from January 2025 to April 2025. This cohort comprised both prospective fresh-tissue samples and retrospective archived paraffin-embedded specimens.

The 5 prospective fresh tissue specimens were collected immediately after surgical resection between January 2025 and April 2025, following prior ethical approval. The 15 paraffin-embedded specimens were retrieved from the hospital-archived pathology tissue bank during the same period under this ethical authorization; the original surgical procedures that generated these paraffin-embedded specimens were performed from October 2023 to April 2025.

In this cohort of 20 patients, 18 were men and 2 were women, with a median age of 62 years (range: 33-80 years), and none had received preoperative chemotherapy, radiotherapy, immunotherapy or other anticancer treatments prior to surgery. Fresh tissue samples were immediately frozen in liquid nitrogen and stored at -80˚C until further analysis. Written informed consent was obtained from each patient before prospective fresh-tissue sampling. Archived paraffin specimens were fully anonymized and de-identified, and the requirement for repeated patient informed consent was waived by the aforementioned ethics committee. All procedures were conducted in accordance with the ethical guidelines outlined in the Declaration of Helsinki.

Patients were eligible if they had postoperatively pathologically confirmed hepatocellular carcinoma, had received no preoperative anticancer treatment and had complete clinical, surgical and pathological records. Patients with a history of other malignancies, prior interventional, ablative or targeted therapy or immunotherapy, non-pure hepatocellular carcinoma (such as cholangiocarcinoma or combined hepatocellular-cholangiocarcinoma), or incomplete clinical or pathological data were excluded.

Pan-cancer expression and survival analysis. Although CENPW upregulation and its prognostic relevance in liver cancer have been reported, those findings were mostly derived from single-center cohorts. The present TIMER2.0-based pan-cancer expression analysis and TCGA-LIHC survival analysis were therefore performed as preliminary exploratory work to profile CENPW expression across multiple cancer types and independently verify its prognostic value in a large public cohort, thereby providing supporting rationale for the subsequent cellular mechanistic experiments. CENPW expression across different cancer types was analyzed using the TIMER2.0 database (http://timer.cistrome.org/). RNA sequencing data and corresponding clinical information for liver cancer were obtained from The Cancer Genome Atlas [TCGA; TCGA-LIHC dataset (22)]. Transcript abundance was normalized to transcript per million values. All statistical analyses and data visualization for this dataset were performed using the Xiantao Academic Bioinformatics Analysis Tool (Helix Group), which is built upon R software (v4.2.1; R Foundation for Statistical Computing; https://www.rproject.org/). The embedded R packages ggplot2 (v3.4.4), stats (v4.2.1) and car (v3.10) were used for plotting and statistical testing. Statistical tests were selected according to the characteristics of the data; analyses were not performed when the assumptions of the chosen test were violated. Differential expression analysis, tumor grade correlation analysis and Kaplan-Meier survival analysis were performed using this tool. Prognostic survival data were obtained from a previously published TCGA-based study (23). These standardized survival metadata were matched to TCGALIHC geneexpression data via patient barcodes and utilized for overallsurvivalrelated survival analyses. Survival analyses were conducted using the Xiantao Academic Bioinformatics Analysis Tool (Helix Group) built on R 4.2.1 with stats (v4.2.1), survival (v3.3.1), survminer (v0.4.9) and ggplot2 (v3.4.4). The Wilcoxon ranksum test compared CENPW expression between HCC and normal liver tissues, and boxplots were generated by ggplot2. Patients were stratified into low and highexpression groups according to median $\log_2$(TPM+1) transformed CENPW values. Overallsurvival differences were evaluated by KaplanMeier and logrank tests. Cox proportionalhazards regression calculated HR and 95% CI, and the cox.zph function was used to examine the proportionalhazards (PH) assumption. Logrank results were prioritized upon PH assumption violation, with HR/95% CI treated as supplementary data. The rigorous RMST alternative for PHviolation was not supported by this tool. All twosided tests adopted $P<0.05$ as the significance threshold.

Immunohistochemistry. Paraffin-embedded tissue sections (4-μm thickness) were obtained from tissues fixed in 4% paraformaldehyde (cat. no. BL539A; Biosharp Life Sciences) at room temperature for 24 h, processed using standard deparaffinization and rehydration through a descending ethanol series (100, 95, 80 and 70% ethanol), followed by antigen retrieval in 0.01 M citrate buffer (pH 6.0) via microwave heating to ~100˚C for four 6min cycles. After cooling and PBS washing, endogenous

peroxidase was quenched with PBS containing 0.3% (v/v) hydrogen peroxide and 0.3% (v/v) Triton X100 at room temperature in the dark for 30 min. Sections were blocked with 5% goat serum (cat. no. G12085ML; Wuhan Servicebio Technology Co., Ltd.) at room temperature for 10-30 min before being subjected to immunohistochemical staining for CENPW (also known as C6ORF173; primary antibody: cat. no. bs15230R; dilution, 1:200; BIOSS). Primary antibody incubation was performed for 1 h at room temperature and then overnight at 4˚C; slides were rewarmed at 37˚C for 45 min after removal from the refrigerator. After five PBS washes (5 min each), HRPconjugated goatantirabbit IgG secondary antibody (cat. no. C030212; dilution, 1:100; Wuhan Servicebio Technology Co., Ltd.) was applied and incubated at 37˚C for 30 min. Following another five PBS washes (5 min each), chromogenic detection was performed using a DAB detection kit with the reaction monitored under light microscopy for 3-10 min. Sections were counterstained with hematoxylin for up to 20 sec, rinsed with tap water, blued in PBS, dehydrated, cleared in xylene and mounted. Sections incubated with PBS instead of primary antibody were used as negative controls. Stained sections were visualized under a light microscope (Olympus) and independently evaluated by two blinded observers.

Cell cultures. The human liver cancer cell lines, MHCC97-H (cat. no. ZQ0020), PLC/PRF/5 (cat. no. ZQ0027), Huh-7 (cat. no. ZQ0025) and HepG2 (cat. no. ZQ0022) were purchased from Shanghai Zhongqiao Xinzhou Biotechnology Co., Ltd. These liver cancer cells were cultured in high-glucose DMEM (cat. no. C11995500BT; Gibco; Thermo Fisher Scientific, Inc.) supplemented with 10% fetal bovine serum (cat. no. A3161001C; Gibco; Thermo Fisher Scientific, Inc.) and 1% penicillin-streptomycin at 37˚C and 5% CO_2. Normal immortalized human liver THLE-2 cells (cat. no. CL-0833) were purchased from Zhejiang Nobo Biological Products Co., Ltd., and maintained in the supplier recommended special complete medium for THLE-2 cells (cat. no. nobcell0548wp; Zhejiang Noble Biological Products Co., Ltd.), which contains 10% fetal bovine serum and 1% penicillinstreptomycin, under identical incubation conditions (37˚C, 5% CO_2).

All the cell lines were STR-authenticated by the supplier before delivery, with official identification records on file. Manufacturer's pre-shipment mycoplasma assays verified that the original cell stocks were contamination free. Strict aseptic handling was implemented throughout the cell culture to avoid secondary contamination.

Small interfering RNA (siRNA)-mediated CENPW knockdown. HepG2 and Huh7 cells were transfected with CENPW-specific siRNAs or negative control siRNA (Shanghai GenePharma Co., Ltd.; Table SI) using GP-transfect-Mate transfection reagent according to the manufacturer's instructions. The siRNA stock solution was 20 μmol/l, and the final working concentration for transfection was 120 nmol/l. GPtransfectMate transfection reagent was obtained from Shanghai GenePharma Co., Ltd. Cells were incubated with transfection complexes at 37˚C under 5% CO_2 for 12 h, followed by replacement with fresh complete medium. Knockdown efficiency was assessed by reverse transcription-quantitative PCR (RT-qPCR) 24 h post transfection and by western blotting 48 h post transfection. The siRNA (si1-CENPW) with the highest knockdown efficiency was used for subsequent experiments. The control group represented untreated cells cultured under standard conditions, with no transfection reagent or siRNA. Both siNC and siCENPW cells were transfected with corresponding siRNAs using GPtransfectMate transfection reagent per the manufacturer's instructions.

Gene expression analysis

RT-qPCR. Total RNA was isolated from cultured hepatocellular carcinoma cells and clinical human HCC as well as paired adjacent nontumor liver tissues using TRIzol LS reagent (cat. no. 10296010CN; Thermo Fisher Scientific, Inc.). Reverse transcription was carried out at 37˚C for 15 min, followed by 85˚C for 5 sec into cDNA using a PrimeScript RT reagent Kit with gDNA Eraser (cat. no. RR047A; Takara Bio, Inc.). qPCR was performed using the TB Green Premix Ex Taq II kit (cat. no. RR820A; Takara Bio, Inc.) on a LightCycler real-time PCR system. The thermocycling conditions were as follows: 1 cycle of pre-denaturation at 95˚C for 30 sec; 40 cycles of denaturation at 95˚C for 5 sec and annealing-extension at 60˚C for 20 sec. A melting-curve analysis was performed at the end of amplification. The primer sequences are listed in Table SII. Relative expression levels were calculated using the $2^{-\Delta\Delta Cq}$ method, with β-actin as the normalization gene (24).

Western blotting. Total protein was extracted from cells or tissues using RIPA buffer (cat. no. P001; Youke Zhuoye Biotechnology Co., Ltd.) supplemented with protease and phosphatase inhibitors. Protein concentration was quantified by BCA assay. Equal quantities of total protein (30 μg per lane) were separated by 10% SDS-PAGE and electro-transferred onto PVDF membranes (MilliporeSigma). Membranes were blocked with 5% non-fat dry milk at room temperature for 1 h, and incubated with primary antibodies against CENPW, phosphorylated YAP (p-YAP), total YAP, E-cadherin, N-cadherin and β-actin overnight at 4˚C. After washing, membranes were incubated with corresponding HRP conjugated secondary antibodies for 1 h at room temperature. Protein bands were visualized using enhanced chemiluminescence substrate (cat. no. WBKLS0500; Merck Millipore). After exposure on Xray film, the film was developed, fixed and scanned. Densitometric quantification of band intensity was performed using ImageJ, version 1.54s (National Institutes of Health) software. Detailed antibody information is listed in Table SIII.

Assessment of cell viability. Cell viability was measured via a Cell Counting Kit-8 colorimetric assay (cat. no. GK1001; GLPBIO Technology LLC) according to the manufacturer's instructions. Transfected cells were seeded into a 96-well plate. After the indicated treatment, CCK8 working solution was added and incubated for 2 h at 37˚C, and the absorbance (optical density) at 450 nm was measured at the indicated time points. The cell viability is expressed as the absorbance value. The control group comprised untreated cells under standard culture conditions, without transfection reagent or siRNA, with all other culture conditions identical to the transfected groups.

Migration and invasion assays. For the woundhealing migration assay, HepG2 and Huh7 human hepatocellular carcinoma cells were seeded into 6well plates and grown until >90% confluency. A straight scratch was created using a sterile 10-μl pipette tip. After scratching, cells were washed twice with PBS and cultured in serumfree DMEM to exclude cell proliferation interference. Images were captured at 0, 24 and 48 h under an inverted light microscope (Olympus Corporation). The wound area was quantified using ImageJ software (version 1.54s; National Institutes of Health). The migration rate was calculated as follows: (0 h wound area-area at the indicated time point)/0 h wound area x100. For the invasion assay, 8 μm pore Transwell inserts were precoated with 50 μl of 1:8 diluted Matrigel at 37˚C for 4 h. A total of 2.5x10^5 transfected cells in 150 μl serumfree DMEM were seeded in the upper chamber; no drug treatment was used for basic invasion assays, whereas CENPWknockdown cells received TRULI pretreatment for rescue experiments. The lower chamber contained 600 μl DMEM supplemented with 10% FBS as a chemoattractant. Plates were incubated at 37˚C with 5% CO_2 for 48 h. Noninvaded cells on the upper membrane were removed with cotton swabs. Invaded cells were fixed in 4% paraformaldehyde (room temperature, 60 min) and stained with 1% crystal violet (room temperature, 15 min). An inverted light microscope (Olympus Corporation) was used for imaging, and the numbers of invasive cells were counted from five random fields per insert. The control group comprised untreated cells under standard culture conditions, without transfection reagent or siRNA, with all other culture conditions identical to the transfected groups.

Cell cycle and apoptosis analysis. The cell cycle distribution was analyzed by propidium iodide (PI; Jiangsu KeyGen Biotech Co., Ltd.) staining followed by flow cytometric analysis. Apoptosis was assessed using Annexin V/PI staining and quantified by flow cytometry. All flow cytometry data were acquired on a BD FACSCanto II flow cytometer (BD Biosciences). Data were analyzed using ModFit LT 4.0 (Verity Software House) for the cell cycle and FlowJo v10.9.0 (BD Biosciences) for cell apoptosis. Representative dot plots with complete visible axis scales are presented in the figures. The control group comprised untreated cells under standard culture conditions, without transfection reagent or siRNA, with all other culture conditions identical to the transfected groups.

Pharmacological rescue assay using TRULI (LatsIN1). TRULI (LatsIN1; cat. no. E1061; Selleck Chemicals), a selective LATS1/2 kinase inhibitor, was dissolved in cell-culturegrade DMSO. Gradient concentrations (1, 5, 10 and 15 μM) were tested for 24 h in CENPWknockdown HepG2 and Huh7 cells to exclude cytotoxicity and identify optimal working doses; 15 μM for HepG2 and 10 μM for Huh7. Cells were divided into siNC, siCENPW and siCENPW + TRULI groups. After 24 h of treatment, RTqPCR and western blotting were performed to detect HippoYAP and EMTrelated molecules. Woundhealing and Transwell invasion assays were used to assess cell migration and invasion.

Statistical analysis. All experiments were performed independently at least three times, and the data are presented as the mean ± SEM. The normality of the data distribution was assessed using the Shapiro-Wilk test prior to subsequent statistical analysis. For comparisons between two groups, a two-tailed unpaired Student's t-test was used. For comparisons among multiple groups, one-way analysis of variance was applied followed by Tukey's post hoc test. All the statistical analyses were performed using GraphPad Prism 8 software (Dotmatics). $P<0.05$ was considered to indicate a statistically significant difference.

Results

CENPW is upregulated in liver cancer and is associated with poor prognosis. To investigate the expression pattern and clinical relevance of CENPW in liver cancer, a pan-cancer expression analysis was first performed using the TIMER2.0 database. Upregulated expression of CENPW was detected across multiple tumor types, including liver hepatocellular carcinoma (Fig. 1A). Analysis of transcriptomic data from TCGA further demonstrated higher expression of CENPW in 374 liver cancer tissues than in 50 normal liver tissues (Fig. 1B). Stratification by tumor grade revealed a progressive increase in CENPW expression with increasing histological grade (Fig. 1C-E). Kaplan-Meier survival analysis revealed that patients with high expression of CENPW had poorer overall survival than those with low expression (Fig. 1F), indicating that elevated CENPW expression is associated with an unfavorable prognosis in patients with liver cancer.

These bioinformatics findings were further validated experimentally. Both the transcript and protein expression levels of CENPW were markedly elevated in liver cancer tissue samples compared with adjacent non-cancerous liver tissue samples (Fig. 1G-I). At the cellular level, CENPW expression was markedly higher in all the tested liver cancer cell lines (HepG2, Huh-7, PLC/PRF/5 and MHCC97-H) than in normal human liver cells (THLE2), with the most prominent expression observed in HepG2 and Huh-7 cells (Fig. 1J and K). These results further confirmed that CENPW is aberrantly upregulated in liver cancer and may be closely associated with tumor progression and poor clinical outcomes.

CENPW knockdown suppresses proliferation and induces apoptosis and S-phase cell cycle arrest in liver cancer cells. Given the high endogenous expression of CENPW in HepG2 and Huh-7 cells, these two cell lines were selected for subsequent loss-of-function studies. To determine the most effective siRNA, HepG2 and Huh-7 cells were transfected with different CENPW-targeting siRNAs. si1-CENPW exhibited the highest knockdown efficiency in both cell lines (Fig. 2A and B) and was used for subsequent experiments; this group is referred to as the si-CENPW group. Efficient knockdown of CENPW expression was confirmed at both the transcript and protein levels (Fig. 2C). The loss of CENPW resulted in significant reductions in cell proliferation in both cell lines (Fig. 2D and E), with HepG2 cells exhibiting greater sensitivity to CENPW knockdown.

Further analysis revealed that growth inhibition following CENPW knockdown was accompanied by a significant increase in the number of apoptotic cells (Fig. 2F-H). In parallel, cell cycle profiling revealed a significant accumulation

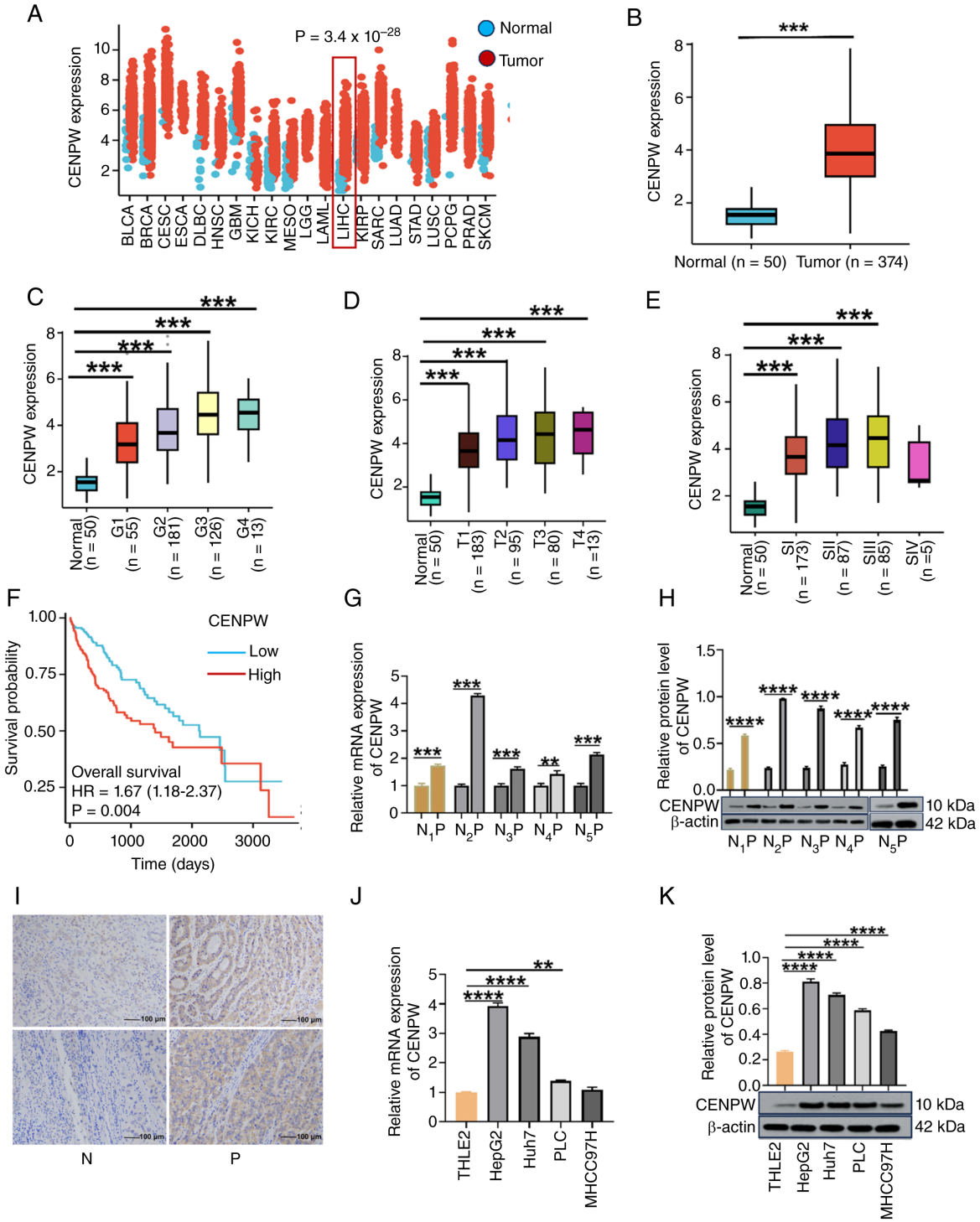


Figure 1. CENPW is upregulated in liver cancer, and its high expression is associated with poor patient survival. (A) The expression of CENPW across pan-cancer datasets. (B) The expression of CENPW in liver cancer transcriptomic datasets. The expression of CENPW in liver cancer across different (C) G, (D) T and (E) S grades. (F) Survival curve analysis revealed that high CENPW expression was significantly associated with poor prognosis in patients with liver cancer. (G) mRNA and (H) protein levels of CENPW in clinical liver cancer tissues and adjacent non-tumor tissues. (I) IHC staining of CENPW in liver cancer and adjacent non-tumor tissues (SP, 10x; scale bar, 100 μm). (J) mRNA and (K) protein expression of CENPW in five cell lines (THLE2: normal liver cell line; HepG2, Huh7, PLC/PRF/5 and MHCC97-H: liver cancer cell lines). IHC, western blot and reverse transcription-quantitative PCR experiments were performed independently at least three times. Data are expressed as the mean ± SEM; n indicates the number of independent biological replicates. **P<0.01, ***P<0.001, ****P<0.0001. CENPW, centromere protein W; LIHC, liver hepatocellular carcinoma; G, histological grade; T, primary tumor stage; S, overall TNM clinical stage; HR, hazard ratio; N, adjacent non-tumor tissue; P, liver cancer tissue; IHC, immunohistochemistry.

of cells in S phase, indicating disruption of normal cell cycle progression (Fig. 2I-K). These findings indicate that CENPW may be essential for the survival of liver cancer cells and that its loss compromises cell viability.

CENPW promotes the migration and invasion of liver cancer cells. Given the association between CENPW expression and advanced tumor grade, its role in liver cancer cell motility was next evaluated. The suppression of CENPW expression

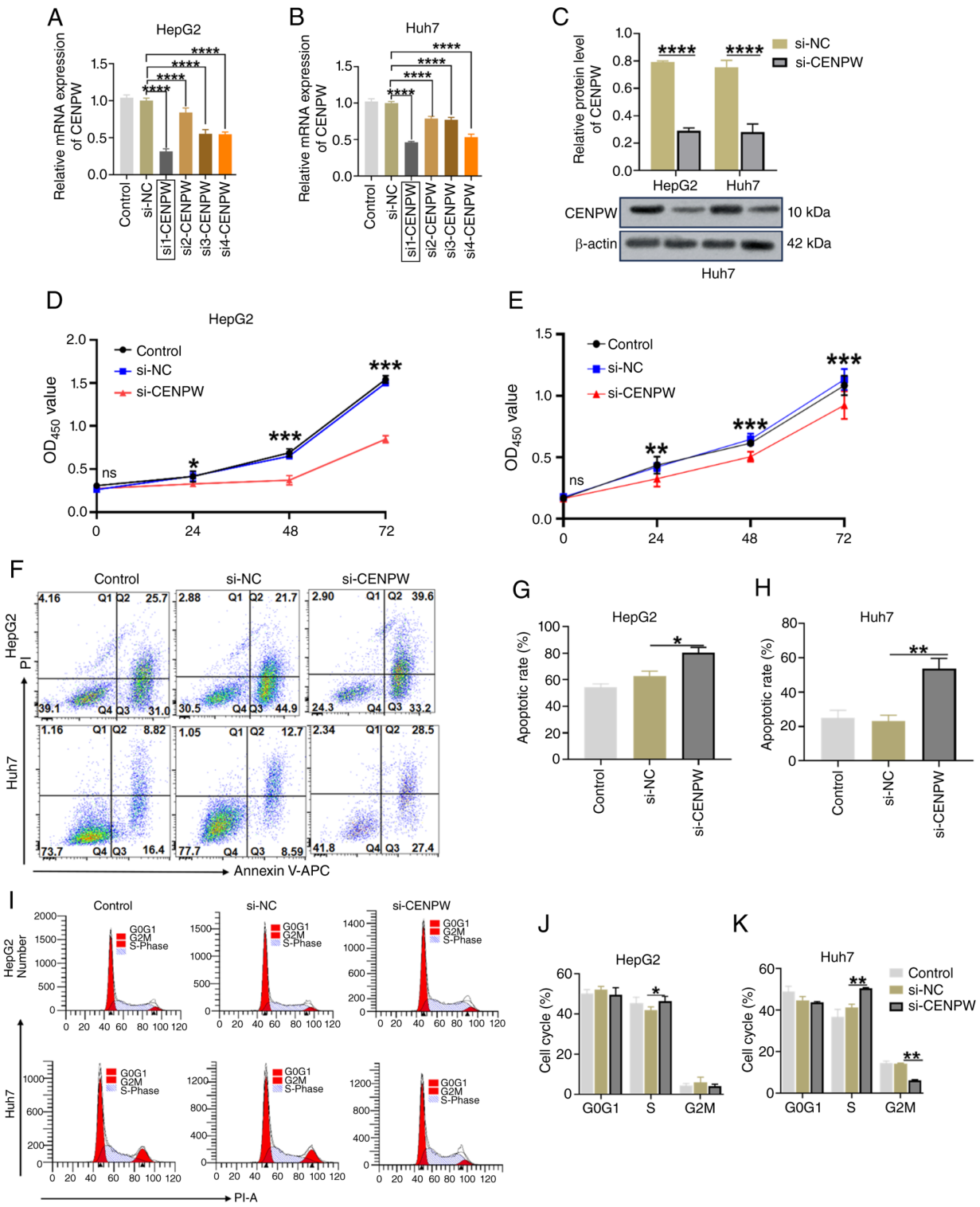


Figure 2. CENPW knockdown inhibits the proliferation of liver cancer cells. HepG2 or Huh7 cells were transfected with different CENPW-targeting siRNAs, and the effects on biological behaviors were evaluated. The mRNA expression of CENPW in (A) HepG2 and (B) Huh7 cells was measured by reverse transcription-quantitative PCR. (C) The protein expression levels of CENPW in HepG2 or Huh7 cells transfected with si1-CENPW were measured by western blotting. The viability of (D) HepG2 or (E) Huh7 cells was assessed using a Cell Counting Kit-8 assay. Apoptosis in HepG2 and Huh7 cells was detected by flow cytometry analysis; (F) representative flow dot plots and pooled statistical data for (G) HepG2 and (H) Huh7 cells are shown (Q1: Necrosis, Q2: Late apoptosis, Q3: Early apoptosis, Q4: Viable). (I) The cell cycle distribution of HepG2 and Huh7 cells was assessed by flow cytometry. The cell cycle distribution of (J) HepG2 and (K) Huh7 cells was quantified. Data are expressed as the mean ± SEM; n=3 for all experiments shown in this figure. *P<0.05, **P<0.01, ***P<0.001, ****P<0.0001. CENPW, centromere protein W; siRNA, small interfering RNA; OD, optical density; NC, negative control; PI, propidium iodide.

significantly impaired the migratory capacity of HepG2 and Huh7 cells, as evidenced by delayed wound closure (Fig. 3A and B). Similarly, the invasive capacity was significantly reduced in response to CENPW knockdown, with fewer cells traversing the Transwell membrane compared with the control cells (Fig. 3C and D). These data indicate that CENPW may

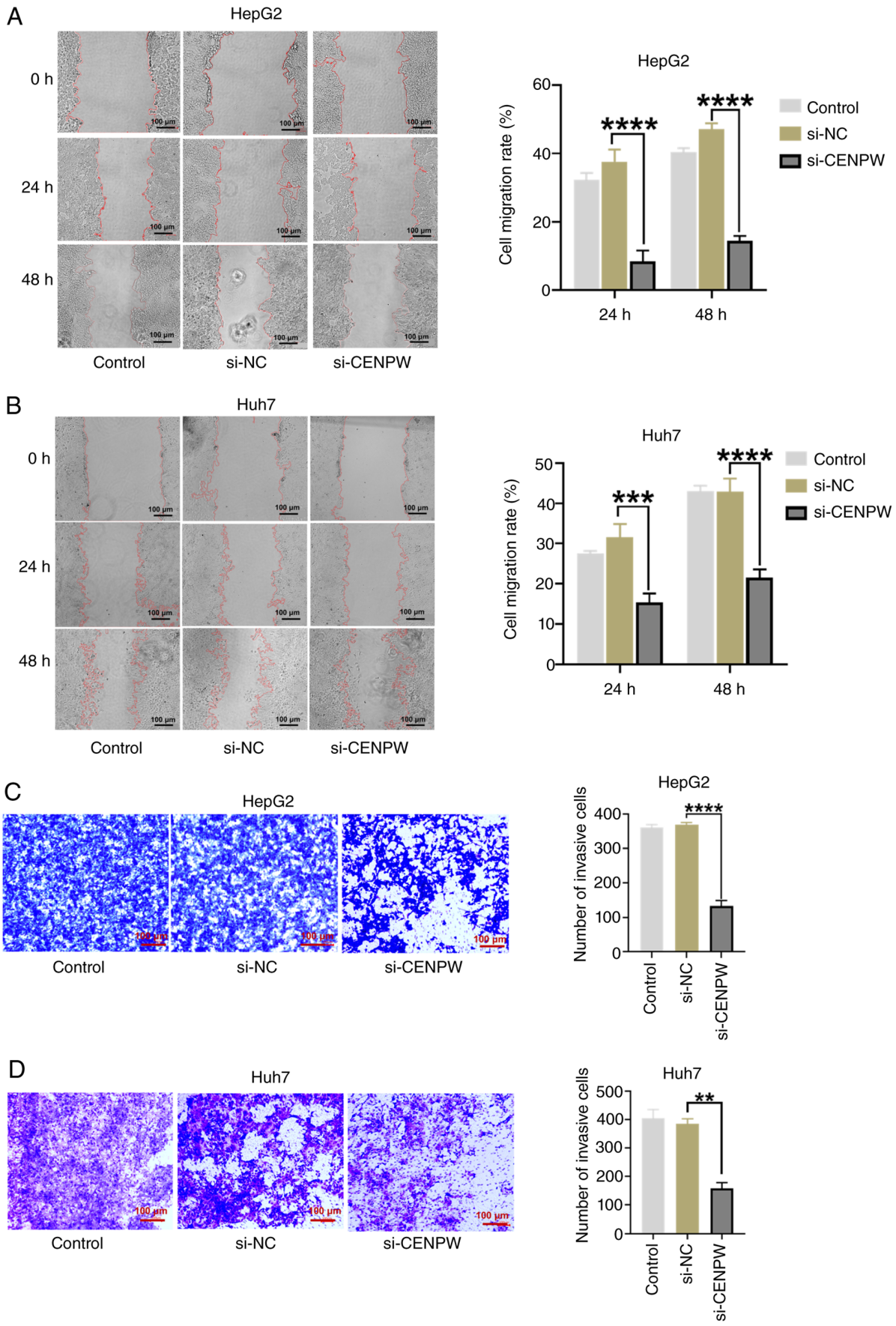


Figure 3. CENPW knockdown inhibits liver cancer cell migration and invasion. Evaluation of the migratory ability of (A) HepG2 and (B) Huh7 cells by wound healing assay (scale bar, 100 μm); representative images and corresponding statistical graphs are shown. Assessment of the invasive abilities of (C) HepG2 and (D) Huh7 cells by Transwell invasion assay (scale bar, 100 μm); representative images and corresponding statistical images are shown. Data are expressed as the mean ± SEM; n=3 for all experiments shown in this figure. **P<0.01, ***P<0.001, ****P<0.0001. CENPW, centromere protein W; siRNA, small interfering RNA; NC, negative control.

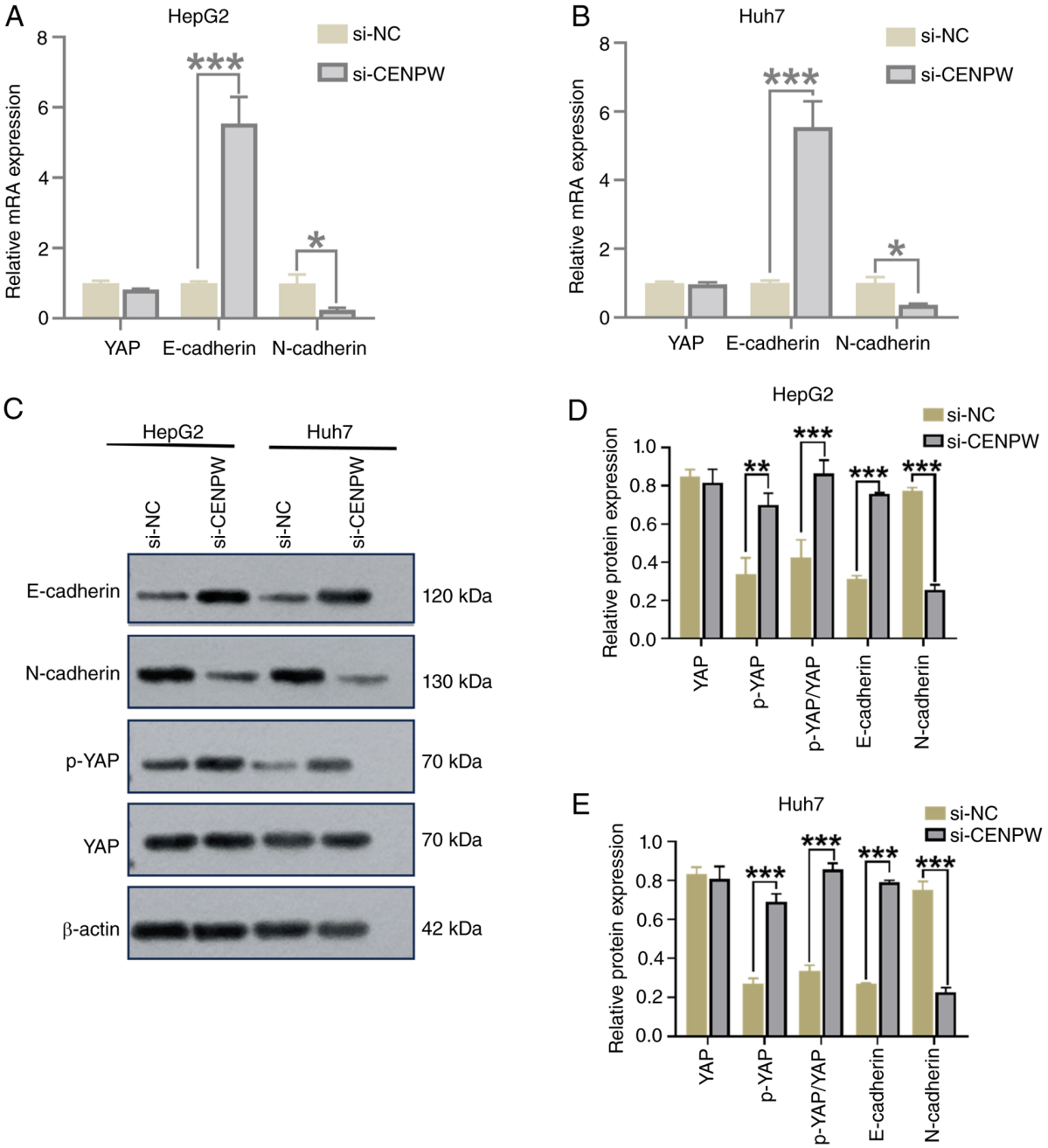


Figure 4. CENPW knockdown suppresses EMT and is associated with the inactivation of YAP signaling. mRNA expression of E-cadherin, N-cadherin and YAP in (A) HepG2 and (B) Huh7 cells was measured by reverse transcription-quantitative PCR. Protein expression of key EMT markers (E-cadherin and N-cadherin) and core Hippo-YAP pathway proteins (p-YAP and YAP) in HepG2 and Huh7 cells was detected by western blotting; (C) representative bands and pooled statistical data for (D) HepG2 and (E) Huh7 cells are shown. Data are expressed as the mean ± SEM; n=3 for all experiments shown in this figure. *P<0.05, **P<0.01, ***P<0.001. CENPW, centromere protein W; EMT, epithelial-mesenchymal transition; siRNA, small interfering RNA; NC, negative control; p-, phosphorylated.

contribute to the migratory and invasive phenotype of liver cancer cells.

CENPW knockdown suppresses EMT and is associated with the inactivation of YAP signaling. To explore the molecular basis underlying the reduction in motility, EMT-associated changes following CENPW knockdown were examined. Loss of CENPW resulted in increased expression of the epithelial marker E-cadherin and decreased expression of the mesenchymal marker N-cadherin in both HepG2 and Huh7 cells (Fig. 4A and B), indicating attenuation of EMT. Concurrently, CENPW knockdown led to a marked increase in p-YAP and an elevated p-YAP/YAP ratio (Fig. 4C-E), which was consistent with reduced YAP transcriptional activity. These molecular changes suggest that suppression of EMT following CENPW loss is accompanied by activation of Hippo signaling and functional inactivation of YAP.

Reactivation of YAP signaling reverses EMT suppression and restores motility in CENPW-knockdown cells. To determine whether Hippo-YAP signaling functionally mediates the effects of CENPW on EMT and cell motility, YAP activity was

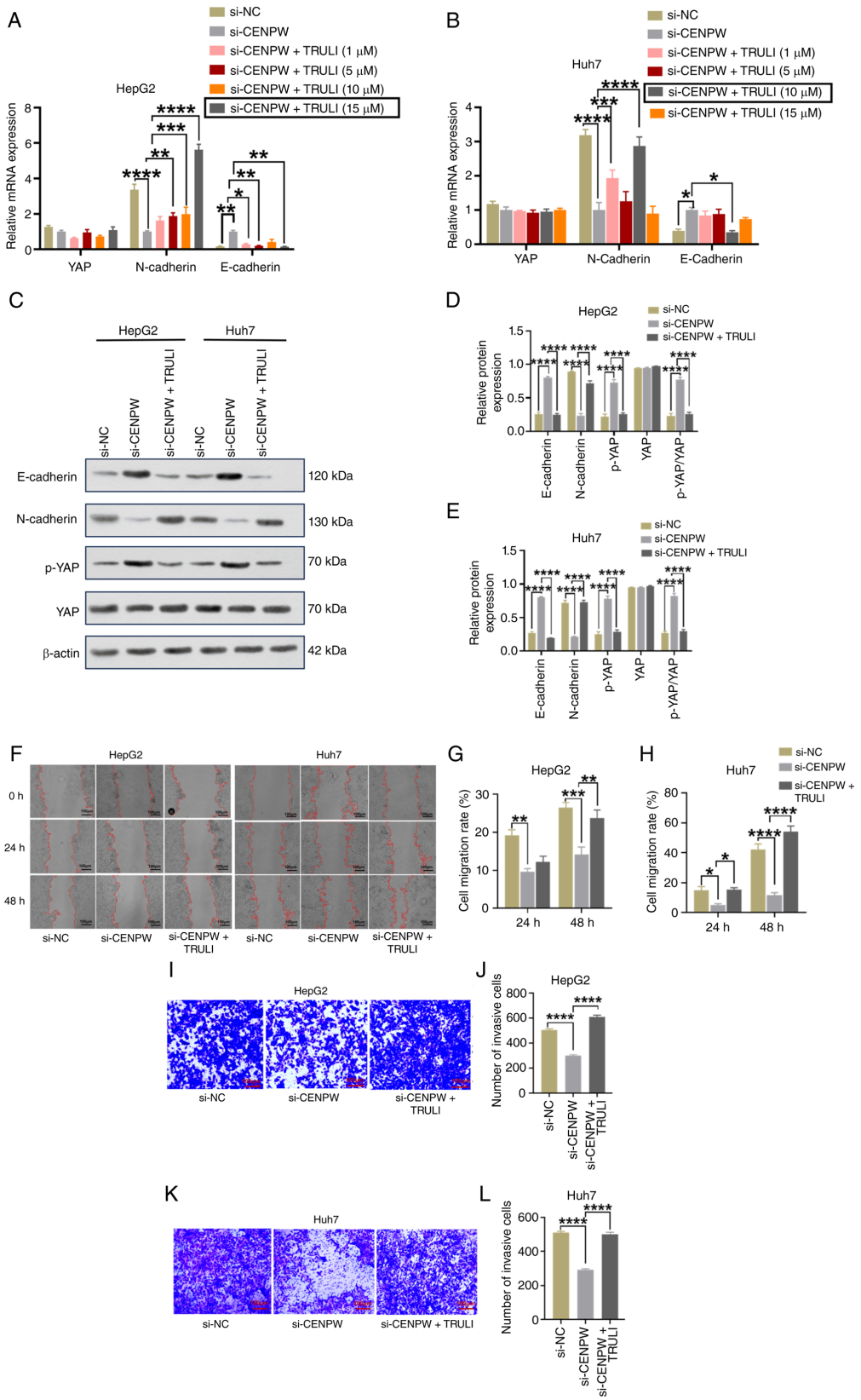


Figure 5. Reactivation of YAP signaling reverses EMT suppression and restores motility in CENPW-knockdown liver cancer cells. CENPW-knockdown HepG2 or Huh7 cells (si-CENPW) were treated with TRULI (1, 5, 10 or 15 μM), and the biological effects were evaluated. The relative mRNA expression of YAP, E-cadherin and N-cadherin in TRULI-treated (A) HepG2 and (B) Huh7 cells was analyzed by RT-qPCR. The relative protein expression of E-cadherin, N-cadherin, YAP and p-YAP in TRULI-treated HepG2 and Huh7 cells was detected by WB; (C) representative bands and pooled statistical data for (D) HepG2 and (E) Huh7 cells are shown. Assessment of cell migratory ability by wound healing assay (scale bar, 100 μm); (F) representative images and pooled statistical data for (G) HepG2 and (H) Huh7 cells are shown. (I-L) Assessment of cell invasive ability by Transwell invasion assay (scale bar, 100 μm). (I) Representative images of Transwell invasion for HepG2 cells; (J) pooled statistical data for HepG2 cell invasion. (K) Representative images of Transwell invasion for Huh7 cells; (L) pooled statistical data for Huh7 cell invasion. WB and RT-qPCR experiments were performed independently at least three times. Data are expressed as the mean ± SEM. *P<0.05, **P<0.01, ***P<0.001, ****P<0.0001. CENPW, centromere protein W; EMT, epithelial-mesenchymal transition; siRNA, small interfering RNA; NC, negative control; p-, phosphorylated; RT-qPCR, reverse transcription-quantitative PCR; WB, western blotting.

pharmacologically restored in CENPW-knockdown cells using the large tumor suppressor kinase (LATS) inhibitor TRULI. Restoration of YAP activity partially reversed EMT-associated changes, as reflected by reduced E-cadherin expression and increased N-cadherin levels (Fig. 5A-E). Additionally, TRULI treatment effectively reduced YAP phosphorylation and decreased the p-YAP/YAP ratio in CENPW-silenced cells (Fig. 5C-E).

Functionally, reactivation of YAP signaling significantly increased the migratory (Fig. 5F-H) and invasive (Fig. 5I-L) capacities of CENPW-knockdown cells, restoring these phenotypes to control levels. Together, these findings indicate that Hippo-YAP signaling may play a functional role in mediating the effects of CENPW on EMT and liver cancer cell motility.

Discussion

The present study identified CENPW as a functionally relevant regulator of malignant phenotypes in liver cancer and provided evidence linking CENPW to Hippo-YAP-mediated control of EMT (25,26). Although CENPW has previously been reported to be upregulated in several cancer types (21,27), its mechanistic role in liver cancer remains unclear.

In the present study, it was demonstrated that CENPW was significantly upregulated in liver cancer tissues and cell lines and that high CENPW expression was associated with advanced tumor grade and poor patient survival, which is consistent with a previous report (14). Beyond expression validation, functional analysis revealed that CENPW knockdown markedly suppressed liver cancer cell proliferation, which was accompanied by increases in apoptosis and S-phase cell cycle arrest. Given the established role of centromere-associated proteins in coordinating chromatin dynamics and cell cycle progression, these findings suggest that loss of CENPW may disrupt cell cycle homeostasis, thereby limiting tumor cell growth.

In the present study, in addition to its role in proliferation, CENPW was found to contribute to liver cancer cell migration and invasion. CENPW knockdown inhibited these processes and was accompanied by altered expression of EMT markers, characterized by increased E-cadherin expression and decreased N-cadherin expression. As EMT is a key driver of tumor invasion, tumor metastasis and therapeutic resistance (28-31), suppression of EMT provides a plausible explanation for the reduced motility observed in cells with CENPW knockdown.

A central novel finding of the present study is the association between CENPW and Hippo-YAP signaling. Numerous studies have shown that the Hippo pathway plays key roles in liver size control and tumorigenesis (32-34). YAP is an important protein downstream of the Hippo pathway. When the Hippo pathway is activated, YAP is phosphorylated by LATS1/2, resulting in elevated levels of p-YAP, which binds to 14-3-3 proteins, thereby inhibiting its entry into the nucleus and suppressing tumor growth. Conversely, inhibition of the Hippo pathway allows unphosphorylated YAP to translocate to the nucleus, where it interacts with TEAD transcription factors to promote tumor growth (35). YAP1 upregulation is not only closely related to tumor occurrence and development but also plays important roles in cell proliferation, invasion, metastasis and drug resistance (36). Consistent with a recent study demonstrating that inhibition of mammalian sterile 20like kinases 1/2 (MST1/2) accelerates hepatocarcinogenesis via ERK/MAPK crosstalk (37). Collectively, the results of the present study suggest that CENPW may modulate the HippoYAP signalling pathway. CENPW knockdown elevated the pYAP/YAP protein ratio, altered the expression profiles of EMTrelated markers, and attenuated the migratory and invasive capacities of liver cancer cells. Pharmacological rescue experiments using TRULI further support this functional association, whereas the detailed upstream regulatory mechanisms involving MST1/2 and YAP nuclear activity remain to be elucidated. It was observed that CENPW knockdown increased YAP phosphorylation and the p-YAP/YAP ratio, which was consistent with reduced YAP activity. These molecular changes coincided with the suppression of proliferation and EMT, suggesting that Hippo signaling may function as a downstream mediator of CENPW activity in liver cancer cells. In addition, pharmacological reactivation of YAP signaling using the LATS kinase inhibitor TRULI partially reversed the EMT-suppressive and antimigratory effects induced by CENPW knockdown, providing functional evidence that YAP contributes to the CENPW-mediated regulation of malignant behavior.

The findings of the present study are also consistent with those of previous reports showing that CENPW (also known as CUG2) promotes EMT through YAP-related mechanisms in lung cancer (21,38), suggesting that CENPW may play a conserved role in regulating tumor cell plasticity. Although the precise molecular link between a centromere-associated protein and Hippo-YAP signaling remains to be elucidated, it is plausible that CENPW influences this pathway indirectly through the perturbation of cell cycle dynamics or chromatin-associated stress.

Several limitations of the present study should be acknowledged. First, the conclusions are based on only *in vitro* cellular experiments and thus need further support through *in vivo* animal studies. Second, the relatively small sample size of the single-center tissue cohort limits how broadly the findings can be applied; thus, further multicenter studies are needed. Critically, the direct molecular interaction between CENPW and Hippo-YAP signaling components has not yet been clarified; Co-immunoprecipitation, GST pull-down and YAP subcellular localization assays are planned for our future work. Furthermore, gain-of-function rescue experiments were not performed as transient transfection of the CENPW plasmid resulted in unstable and inconsistent overexpression efficiency. To address this, stable overexpression models will be established in future and then a full set of functional tests (proliferation, migration, invasion and EMT) will be carried out to confirm the oncogenic role of CENPW. Finally, the pharmacological rescue experiments using TRULI lacked serial doseresponse assessments and a dedicated DMSO solventcontrol group. Therefore, conclusions drawn from TRULIinduced YAP reactivation should be interpreted with caution. Full doseresponse assays with strictly matched DMSO solvent controls will be performed in future investigations.

In conclusion, the present study demonstrated that CENPW is aberrantly upregulated in liver cancer and may be associated with tumor cell proliferation, EMT, migration and

invasion. These effects may be associated with the modulation of Hippo-YAP signaling, highlighting a previously underexplored link between centromere-associated proteins and oncogenic signaling pathways. These findings identify CENPW as a potential biomarker and therapeutic target for liver cancer and provide a framework for future mechanistic investigations.

Acknowledgements

The authors would like to thank Mr. Long Ping from the Department of Clinical Laboratory, Qiannan People's Hospital (Duyun, China) for technical guidance, Ms. Jiuwen Tang from the Department of Pathology, Qiannan People's Hospital for assistance with specimen collection, and Ms. Jing Li from the Center for Clinical Laboratory, the Affiliated Hospital of Guizhou Medical University (Guiyang, China) for expert guidance on the experimental procedures.

Funding

The present study was supported by the Research Project of Qiannan Medical College for Nationalities (grant no. Qnyz2024021) and the Health Science and Technology Research Projects of Guizhou Provincial Health Commission (grant nos. gzwkj2026-239 and gzwkj2024-467).

Availability of data and materials

The data generated in the present study may be requested from the corresponding author.

Authors' contributions

FY and YW conceived and designed the study. XF and LW acquired and analyzed the data and drafted the manuscript. HY acquired experimental data and critically revised the manuscript. YQ performed data interpretation and critically revised the manuscript. JZ contributed to the conception of the study, interpreted the data and critically revised the manuscript. FY also oversaw the study, performed statistical analysis and assisted in drafting the Methods section. FY, XF and YW confirm the authenticity of all the raw data. All authors were accountable for all aspects of the work. All authors have read and approved the final version of the manuscript.

Ethics approval and consent to participate

The present study was reviewed at the ethics committee meeting on December 12, 2024 and formally approved on December 27, 2024 (approval no. 2025-qnzy-13). Sample collection and archived paraffin-embedded specimen retrieval for the present study were performed from January 2025 to April 2025 after obtaining the aforementioned ethical approval. Written informed consent was obtained from all patients who provided fresh prospective tissue samples. The ethics committee waived the requirement for repeated informed consent for anonymized retrospective paraffin-embedded archived specimens. All experimental procedures complied with the principles of the Declaration of Helsinki.

Patient consent for publication

Not applicable.

Competing interests

The authors declare that they have no competing interests.

Use of artificial intelligence tools

During the preparation of this work, artificial intelligence tools were used to improve the readability and language of the manuscript, and subsequently, the authors revised and edited the content produced by the artificial intelligence tools as necessary, taking full responsibility for the ultimate content of the present manuscript.

References

1. Bray F, Laversanne M, Sung H, Ferlay J, Siegel RL, Soerjomataram I and Jemal A: Global cancer statistics 2022: GLOBOCAN estimates of incidence and mortality worldwide for 36 cancers in 185 countries. CA Cancer J Clin 74: 229-263, 2024.
2. Ganesan P and Kulik LM: Hepatocellular carcinoma: New developments. Clin Liver Dis 27: 85-102. 2023.
3. Allemani C, Matsuda T, Di Carlo V, Harewood R, Matz M, Nikšić M, Bonaventure A, Valkov M, Johnson CJ, Estève J, *et al*: Global surveillance of trends in cancer survival 2000-14 (CONCORD-3): Analysis of individual records for 37 513 025 patients diagnosed with one of 18 cancers from 322 population-based registries in 71 countries. Lancet 391: 1023-1075, 2018.
4. Arnett A, Siegel DA, Dai S, Thompson TD, Foster J, di Pierro EJ, Momin B, Lupo PJ and Heczey A: Incidence and survival of pediatric and adult hepatocellular carcinoma, United States, 2001-2020. Cancer Epidemiol 92: 102610, 2024.
5. Lee S, Gang J, Jeon SB, Choo SH, Lee B, Kim YG, Lee YS, Jung J, Song SY and Koh SS: Molecular cloning and functional analysis of a novel oncogene, cancer-upregulated gene 2 (CUG2). Biochem Biophys Res Commun 360: 633-639, 2007.
6. Hori T, Amano M, Suzuki A, Backer CB, Welburn JP, Dong Y, McEwen BF, Shang WH, Suzuki E, Okawa K, *et al*: CCAN makes multiple contacts with centromeric DNA to provide distinct pathways to the outer kinetochore. Cell 135: 1039-1052, 2008.
7. Zhang P, Yang Q, Chen X, Chen X, Wang Q, Chen K, An Y, Jiang K and Sun F: CENPW knockdown inhibits progression of bladder cancer through inducing cell cycle arrest and apoptosis. J Cancer 15: 858-870, 2024.
8. Li L, Qi ST, Sun QY and Chen SL: CENP-A regulates chromosome segregation during the first meiosis of mouse oocytes. J Huazhong Univ Sci Technolog Med Sci 37: 313-318, 2017.
9. Liu X and Liu Y: Comprehensive analysis of the expression and prognostic significance of the CENP family in breast cancer. Int J Gen Med 14: 3471-3482, 2022.
10. Shao C, Wang Y, Duan H, Ding P, Zhang Y, Ning J, Han J, Jiang T and Yan X: Mitosis-related gene *CENP-U* as a potential biomarker in malignancy. Ann Transl Med 9: 1744, 2021.
11. Wang Y, Chen J, Meng W, Zhao R, Lin W, Mei P, Xiao H and Liao Y: A five-gene expression signature of centromeric proteins with prognostic value in lung adenocarcinoma. Transl Cancer Res 12: 273-286, 2023.
12. Wang J, Liu X, Chu HJ, Li N, Huang LY and Chen J: Centromere protein I (CENP-I) is upregulated in gastric cancer, predicts poor prognosis, and promotes tumor cell proliferation and migration. Technol Cancer Res Treat 20: 15330338211045510, 2021.
13. He K, Xie M, Li J, He Y and Yin Y: CENPO is associated with immune cell infiltration and is a potential diagnostic and prognostic marker for hepatocellular carcinoma. Int J Gen Med 15: 7493-7510, 2022.
14. Zhou Y, Chai H, Guo L, Dai Z, Lai J, Duan J, Liu Y and Ding Q: Knockdown of CENPW inhibits hepatocellular carcinoma progression by inactivating E2F signaling. Technol Cancer Res Treat 20: 15330338211007253, 2021.

15. Zhou Z, Zhou Z, Huang Z, He S and Chen S: Histone-fold centromere protein W (CENP-W) is associated with the biological behavior of hepatocellular carcinoma cells. Bioengineered 11: 729-742, 2020.
16. Yang Z, Chen W, Liu Y and Niu Y: Recent updates of centromere proteins in hepatocellular carcinoma: A review. Infect Agent Cancer 20: 7, 2025.
17. Wang G, Zhang J, Li Y, Zhang Y, Dong W, Wu H, Wang J, Liao P, Yuan Z, Liu T and He W: Integrating single-cell RNA sequencing, WGCNA, and machine learning to identify key biomarkers in hepatocellular carcinoma. Sci Rep 15: 11157, 2025.
18. Papavassiliou KA, Sofianidi AA and Papavassiliou AG: YAP/TAZ-TEAD signalling axis: A new therapeutic target in malignant pleural mesothelioma. J Cell Mol Med 28: e18330, 2024.
19. Cheng J, Wang S, Dong Y and Yuan Z: The role and regulatory mechanism of hippo signaling components in the neuronal system. Front Immunol 11: 515462, 2020.
20. Park H, Lee Y, Lee K, Lee H, Yoo JE, Ahn S, Park YN and Kim H: The clinicopathological significance of YAP/TAZ expression in hepatocellular carcinoma with relation to hypoxia and stemness. Pathol Oncol Res 27: 604600, 2021.
21. Kaowinn S, Yawut N, Koh SS and Chung YH: Cancer upregulated gene (CUG)2 elevates YAP1 expression, leading to enhancement of epithelial-mesenchymal transition in human lung cancer cells. Biochem Biophys Res Commun 511: 122-128, 2019.
22. Cancer Genome Atlas Research Network. Electronic address: wheeler@bcm.edu; Cancer Genome Atlas Research Network: Comprehensive and integrative genomic characterization of hepatocellular carcinoma. Cell 169: 1327 1341.e23, 2017.
23. Wu R, Deng X, Wang X, Li S, Su J and Sun X: Prognostic factors and risk prediction model for hepatocellular carcinoma based on TCGA database. J Clin Med 7: 562, 2018.
24. Livak KJ and Schmittgen TD: Analysis of relative gene expression data using real-time quantitative PCR and the 2(-Delta Delta C(T)) method. Methods 25: 402-408, 2001.
25. Pol S: Carcinome hépatocellulaire (CHC). Med Trop Sante Int 4: mtsi.v4i4.2024.614, 2024.
26. Wang W and Wei C: Advances in the early diagnosis of hepatocellular carcinoma. Genes Dis 7: 308-319, 2020.
27. Yang P, Pei X, Deng J and Li X: Comprehensive analysis of centromere protein family member genes in lung adenocarcinoma. Crit Rev Eukaryot Gene Expr 32: 57-72, 2022.
28. Pal M, Bhattacharya S, Kalyan G and Hazra S: Cadherin profiling for therapeutic interventions in epithelial mesenchymal transition (EMT) and tumorigenesis. Exp Cell Res 368: 137-146, 2018.
29. Brabletz S, Schuhwerk H, Brabletz T and Stemmler MP: Dynamic EMT: A multi-tool for tumor progression. EMBO J 40: e108647, 2021.
30. Huang Z, Zhou L, Duan J, Qin S, Jiang J, Chen H, Wang K, Liu R, Yuan M, Tang X, *et al*: Oxidative stress promotes liver cancer metastasis via RNF25-mediated E-cadherin protein degradation. Adv Sci (Weinh) 11: e2306929, 2024.
31. Huang Y, Hong W and Wei X: The molecular mechanisms and therapeutic strategies of EMT in tumor progression and metastasis. J Hematol Oncol 15: 129, 2022.
32. Li X, Kuang S, Zhang Y, Song T, Hu L, Liu Y, Ramaswamy HS and Yu Y: Zheng Gan Decoction inhibits diethylnitrosamine-induced hepatocellular carcinoma in rats by activating the Hippo/YAP signaling pathway. Nan Fang Yi Ke Da Xue Xue Bao (Chinese) 45: 799-809, 2025.
33. Driskill JH and Pan D: The hippo pathway in liver homeostasis and pathophysiology. Annu Rev Pathol 16: 299-322, 2021.
34. Manmadhan S and Ehmer U: Hippo signaling in the liver-A long and ever-expanding story. Front Cell Dev Biol 7: 33, 2019.
35. Fu M, Hu Y, Lan T, Guan KL, Luo T and Luo M: The Hippo signalling pathway and its implications in human health and diseases. Signal Transduct Target Ther 7: 376, 2022.
36. Wang G, Pang Y, Li N, Hui Y and Jin D: CXCR7 promoted proliferation, migration and invasion in HCC cells by inactivating Hippo-YAP signaling. Discov Oncol 16: 561, 2025.
37. Li M, Xu J, Zhu L, Yang X, Ren H, Jiang J, Li L, Yang Y and Gong Y: Inhibition of MST1/2 attenuates the anti-hepatocarcinogenesis effect of salvianolic acid B via the ERK/MAPK signaling pathway. Eur J Pharmacol 1030: 179156, 2026.
38. Kaowinn S, Kim J, Lee J, Shin DH, Kang CD, Kim DK, Lee S, Kang MK, Koh SS, Kim SJ, *et al*: Cancer upregulated gene 2 induces epithelial-mesenchymal transition of human lung cancer cells via TGF-β signaling. Oncotarget 8: 5092-5110, 2017.

Copyright © 2026 Feng et al. This work is licensed under a Creative Commons Attribution-NonCommercial-NoDerivatives 4.0 International (CC BY-NC-ND 4.0) License.